Mem. Fac. Integrated Arts and Sci., Hiroshima Univ., Ser. IV, Vol. 29 1-25, Dec. 2003

Brain Atlas of the Japanese Eel: Comparison to Other Fishes

T. Mukuda[1, 2] and M. Ando[1]*

[1] *Laboratory of Integrative Physiology, Faculty of Integrated Arts and Sciences, Hiroshima University, Higashi-Hiroshima 739-8521, Japan.*

[2] *Division of Morphological Analysis, Department of Functional, Morphological and Regulatory Sciences, Faculty of Medicine, Tottori University, Yonago, Tottori 683-8503, Japan.*

ABSTRACT

The whole brain atlas of the eel was constructed in the first place by Klüver-Barréra's staining. Eighty one nuclei and thirty fiber tracts were identified in the present study. Basically, the brain topology of the eel was similar to that of the rainbow trout, the goldfish, the zebrafish, and the catfish. However, some details differed from those of other teleosts. The parvocellular preoptic nucleus (PP) was not subdivided, whereas the anterior PP is distinguished from the posterior part in the zebrafish and the rainbow trout. The intermediate thalamic nucleus was not distinguished, whereas it is identified in the zebrafish, the goldfish, and the rainbow trout. The paraventricular organ (PVO) was single, while paired PVOs are observed in the zebrafish. The torus semicircularis (TS) was smaller than that in the goldfish and rainbow trout. The cell size of the nucleus of medial longitudinal fascicle (NMLF) in the tegmentum was larger than that in the glass knifefish and the zebrafish. The protrusion of the nucleus lateralis valvulae (NLV) into the mesencephalic ventricle (VMes) was larger than that in the zebrafish and the rainbow trout. The valvula cerebelli was smaller than those in the goldfish and the zebrafish. The facial lobes (LVII) ran through the medulla oblongata (MO), whereas the two lobes fuse at the caudal cerebellum in the goldfish, the catfish, and the zebrafish. The expansion of the vagal lobe (LX) in the caudal MO was smaller than that in the goldfish and the zebrafish. The glossopharyngeal motor nucleus (MNIX) and the vagal motor nucleus (MNX) were fused to make a columnar structure named glossopharyngeal-vagal motor complex (GVC). Such a columnar complex seems to be common in fishes, since similar columns are observed in the lamprey, the elasmobranch and other teleost fishes. The facial motor nucleus (MNVII) was separated from the GVC, whereas it is fused with the GVC in the sturgeon, the reedfish and the tarpon.

Key words: brain atlas; external morphology; Klüver-Barréra's staining; Japanese eel; glossopharyngeal-vagal motor complex

INTRODUCTION

Maintenance of body fluid homeostasis is essential to life for vertebrates. Especially, drinking behavior is most important for terrestrial vertebrates and marine teleosts to compensate for water loss. However, the neu-

* Corresponding author: Tel. +81-824-24-6569; Fax +81-824-24-0759. E-mail: mando@hiroshima-u.ac.jp
Received October 1 2003; Accepted November 1 2003

ronal control of drinking behavior is not clarified even in mammals (Bourque *et al*., 1994; Fitzsimons, 1998; Takei, 2000). In mammals, after perception of thirst they must first seek for water, which is then ingested and finally swallowed. Furthermore, the neuronal networks of thermo- and osmo-regulation seem to be overlapped in mammals (Takahashi *et al*., 2001). In contrast, fish can swallow immediately following thirst perception, since they live in water and water is constantly held in the mouth for respiration. Therefore, the neuronal circuit for controlling drinking behavior in fish may be less complex, and fish can be expected as a suitable model system to analyze regulatory mechanisms in drinking behavior.

Until now, drinking behavior in fish has been analyzed only in eels (Hirano, 1974; Takei *et al*., 1979, 1998; Ando and Nagashima, 1996; Ando *et al*., 200a, b; Kozaka *et al*., 2003). However, few morphological studies are performed in the eel, whereas a partial description of brain morphology has been reported in the European eel in relation to audition (Meredith and Roberts, 1986, 1987; Meredith *et al*., 1987) or to vision (Wullimann *et al*., 1991). Immunohistochemical studies show the configuration of dopaminergic and cholinergic neurons in the European eel (Roberts *et al*., 1989; Molist *et al*., 1993). In relation to the drinking behavior, anyway, no morphological studies are performed.

Because brain atlas is indispensable to analyze for any behaviors, the present study aims to construct a comprehensive whole brain atlas in the Japanese eel. By constructing the whole brain atlas, we identified eighty one nuclei and thirty fiber tracts following the previous reports in various teleosts: the European eel (Meredith and Roberts, 1986, 1987; Meredith *et al*., 1987; Roberts *et al*., 1989; Wullimann *et al*., 1991; Molist *et al*., 1993), the rainbow trout (Meek and Nieuwenhuys, 1998), the gray mullet (Díaz-Regueira and Anadón, 1992), the goldfish (Peter and Gill, 1975; Morita and Finger, 1987a, b; Goehler and Finger, 1992), the zebrafish (Wullimann *et al*., 1996), the catfish (Kanwal and Caprio, 1987), or other teleosts (Meek and Nieuwenhuys, 1998). The nomenclature of the nuclei and the fiber tracts corresponded to Wullimann *et al*. (1996) and Meek and Nieuwenhuys (1998).

Although the basic topology of the eel brain was similar to those of rainbow trout (Meek and Nieuwenhuys, 1998), the goldfish (Peter and Gill, 1975; Morita and Finger, 1987a, b; Goehler and Finger, 1992; Meek and Nieuwenhuys, 1998), the zebrafish (Wullimann *et al*., 1996), and the catfish (Kanwal and Caprio, 1987), some details differed from those in other teleosts.

MATERIALS AND METHODS

KLÜVER-BARRÉRA 'S STAINING

Cultured Japanese eels *Anguilla japonica*, weighting approximately 200 g, obtained from a commercial source, were acclimated to artificial seawater for a week at 20˚C. After decapitation, the muscular tissues surrounding the skull were removed. The skull was fenestrated bilaterally to allow the fixative to infiltrate effectively into the brain, and immediately immersed into 4 % paraformaldehyde (PFA; Kanto Chemical, Tokyo, Japan) in 0·1 M phosphate buffer (PB; pH 7·4) for 12 h at 4˚C. After fixation, the brain was isolated from the skull. The fixed brain was dehydrated with an ethanol series, cleared with xylene, and embedded in paraffin. Both transverse and sagittal sections were made at 7 μm thickness with a microtome. The sections were stained with the modified method of Klüver and Barréra (1953). Briefly, after removing paraffin, the sections were rinsed with distilled water (DW), and immersed in acetic acid solution (approximately 20 drops of 10 % acetic acid in 100 ml DW) for 5 min, and in 95 % ethanol. The sections were, then, incubated in Luxol Fast Blue MSB

(LFB; Chroma-Gesellschaft, Könger, Germany) solution (1·0 g LFB in 1000 ml of 95 % ethanol) for 24 h at 58˚C. After rinsing in 95 % ethanol, followed by DW, they were differentiated in 0·05 % lithium carbonate for a few seconds at room temperature (RT), and immersed in 70 % ethanol 5 times. The sections were subsequently incubated in Cresyl Violet (CV; Katayamakagaku, Tokyo, Japan) solution (0·1 g CV and a few drops of 10 % acetic acid in 10 ml DW, then filtered prior to incubation) for approximately 30 min at RT. After rinsing in DW, they were dehydrated with ethanol series, cleared with xylene, and coverslipped. The stained slides were examined with an optical microscope (BH-2, Olympus, Tokyo, Japan) equipped with color digital camera (Dimage EX, Minolta, Tokyo, Japan).

RESULTS

EXTERNAL MORPHOLOGY

The external brain morphology of the Japanese eel is shown in Fig. 1. The eel brain extended rostrocaudally with approximately 10 mm long. In the lateral view, four dorsal expansions were distinguished rostrocaudally; the olfactory bulb (OB), the telencephalon (Tel), the optic tectum (TeO) and the cerebellum (Ce). The size of these expansions was nearly equal except for the OB being relatively small. The OB of the eel was close to the Tel, which was rostrocaudally long and ellipsoidal shape. At the level of the TeO, the brain stem was protuberated ventrolaterally, forming the inferior lobe (IL) of the hypothalamus. The eel medulla oblongata (MO) shifted gradually to the spinal cord, whereas the boundary between the MO and the spinal cord was obscure. Ten cranial nerves (I, olfactory; II, optic; III, oculomotor; IV, trochlear; V, trigeminal; VI, abducens; VII, facial; VIII, octaval; IX, glossopharyngeal; X, vagal) and a few spino-occipital nerves (SO) were distinguished.

In a dorsal view, the OB, the Tel and the TeO consisted of paired hemispheres, while the caudal margin of the Ce was subdivided into 3 lobes by two sulci. Caudally to the Ce, the fourth ventricle (V4) existed as a deep and long excavation. More caudally, the area postrema (AP) was identified as a shallow excavation elongated from the MO to the spinal cord. The lateral walls of the AP were reddish in intact brain. In a ventral view, the saccus vasculosus (SV) appeared as a single red disk-like structure (1 mm) situated caudally to the IL.

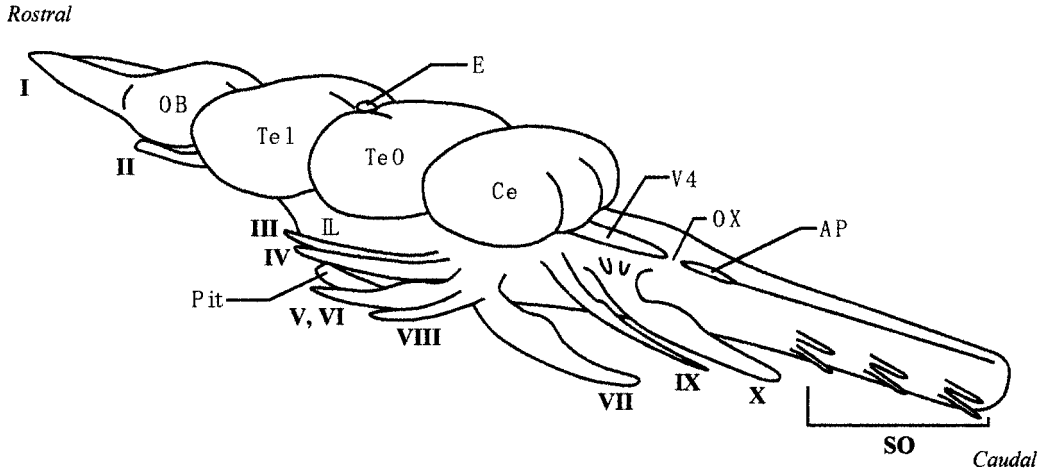

Fig. 1. External morphology of the eel brain (left lateral view). The length from the olfactory bulb (OB) to the area postrema (AP) was approximately 10 mm. All names are abbreviated as shown in Table 1.

Table 1. Abbreviation of nuclei and nerve fibers used in the present study

Abbreviation	Nomenclature	Appearance in Fig. 1-2 Area	Plane	Abbreviation	Nomenclature	Appearance in Fig. 1-2 Area	Plane
A	anterior thalamic nucleus	Die	6	LPM	nucleus lateralis profundus	Mes	12
ALL	anterior lateral line nerve	Rho	17-19	LVII	facial lobe	Rho	20-23
AON	anterior octaval nucleus	Rho	17	LX	vagal lobe	Rho	24-26
AP	area postrema	Rho	27	MaON	magnocellular octaval nucleus	Rho	19
Cans	ansulate commissure	Mes	11,12	MC	Mauthner cell	Rho	17
Cant	anterior commissure	Tel	4	Mes	mesencephalon		
CC	crista cerebellaris	Rho	17-25	MFB	median forebrain bundle	Tel,Die	4-6
Ccer	cerebellar commissure	Rho	15-18	MLF	medial longitudinal fascicle	Mes,Rho	10-27
Ce	cerebellum	Rho		MNIII	oculomotor nucleus	Mes	11,12
Chor	horizontal commissure	Die,Mes	6-9	MNIV	trochlear nucleus	Mes	13
CM	corpus mamillare	Die	11	MNV	trigeminal motor nucleus	Rho	15-17
CO	optic chiasm	Die	5	MNVII	facial motor nucleus	Rho	21-23
CP	dorsal central thalamic nucleus	Die	7-9	MNX	vagal motor nucleus	Rho	
CPN	central pretectal nucleus	Die	8	MO	medulla oblongata	Rho	
Cpop	postoptic commissure	Die	6	MON	medial octavolateral nucleus	Rho	17-23
Cpost	posterior commissure	Die	7-9	MOT	medial olfactory tract	OB,Tel	2-3
Ctec	commissura tecti	Mes	8,9	NAT	anterior tuberal nucleus	Die	7-10
Cven	commissura ventralis rhombencephali	Rho	14-27	NCC	commissural nucleus of the Cajal	Rho	27
				NDV	nucleus of the descending trigeminal root		18,19
D	dorsal telencephalic area	Tel	2-5				
Dc	central zone of the D	Tel	3,4	NFM	medial funicular nucleus	Rho	27
Dd	dorsal zone of the D	Tel	3,4	NI	nucleus isthmi	Rho	13,14
Die	diencephalon			NIn	interpeduncular nucleus	Mes	13
DIL	diffuse nucleus of the inferior lobe	Die	7-12	NLV	nucleus lateralis valvula cerebelli	Mes	11-14
Dl	lateral zone of the D	Tel	3	NMLF	nucleus of the MLF	Mes	10
Dld	dorsal part of the Dl	Tel	4	NPT	postreior tuberal nucleus	Die	11
Dlv	ventral part of the Dl	Tel	4	NR	nucleus ruber	Mes	9,10
Dm	medial zone of the D	Tel	3,4	NRL	nucleus recessi lateralis	Die	8-12
DON	descending octaval nucleus	Rho	20-23	NSO	spinooccipital motor nucleus	Rho	26,27
DOT	dorsomedial optic tract	Die	6,7	NTL	nucleus tori lateralis	Die	7-9
DP	dorsal posterior thalamic nucleus	Die	7-9	OB	olfactory bulb	Tel	
DV	descending trigeminal root	Rho	15-27	OEN	octavolateral efferent nucleus	Rho	20-23
E	epiphysis	Die	5,6	OS	superior olive	Rho	17
ECL	external cellular layer	OB	1	OT	optic tract	Die	5
EG	granular eminence	Rho	15-22	OX	obex	Rho	
EW	Edinger-Westphal nucleus	Mes	12	OVLT	vascular organ of the lamina terminalis	Die	4
FR	fasciculus retroflexus	Die,Mes	7-12				
GL	glomerular layer	OB	1	PCN	paracommissural nucleus	Die	8
GVC	glossopharyngeal-vagal motor complex	Rho	24-27	PG	preglomerular complex	Die	7-10
Ha	habenular nucleus	Die	5,6	PGZ	periventricular gray zone of the optic tectum	Mes	7-15
Had	dorsal habenular nucleus	Die	6				
Hav	ventral habenular nucleus	Die	5,6	Pit	pituitary		
ICL	internal cellular layer	OB	1	PLL	posterior lateral line nerve	Rho	20-23
IL	inferior lobe of the hypothalamus	Die		PM	magnocellular preoptic nucleus	Die	5
INF	infundibulum	Die	8-10	PP	parvocellular preoptic nucleus	Die	4-6
LC	locus coeruleus	Rho	13,14	PPd	dorsal part of the periventricular pretectal nucleus	Die	8,9
LFB	lateral forebrain bundle	Tel,Die	4-6				
LLF	lateral longitudinal fascicle	Mes,Rho	10-16	PPv	ventral part of the periventricular pretectal nucleus	Die	8,9
LOT	lateral olfactory tract	OB,Tel	2				

Continued

Abbreviation	Nomenclature	Appearance in Fig. 1-2 Area	Plane	Abbreviation	Nomenclature	Appearance in Fig. 1-2 Area	Plane
PSp	parvocellular superficial	Die	7	TTBc	tractus tectobulbaris cruciatus	Rho	14-22
	pretectal nucleus			TVS	vestibulo-spinal tract	Rho	15-27
PVO	paraventricular organ	Die	8,9	V	ventral telencephalic area	Tel	2-4
RF	reticular formation	Mes,Rho	13-27	V3	third ventricle	Die	4-9
Rho	rhombencephalon			V4	fourth ventricle	Rho	13-26
RInf	inferior raphe nucleus	Rho	21-26	Vas	vascular lacuna of area postrema	Mes	10,11
RInt	intermediate raphe nucleus	Rho	19-20	Vd	dorsal nucleus of the V	Tel	2,3
RL	recess lateralis	Die	9-11	Vl	lateral nucleus of the V		
RS	superior raphe nucleus	Rho	14	VL	ventrolateral thalamic nucleus	Die	2
RT	rostral tegmental nucleus	Mes	10	VM	ventromedial thalamic nucleus	Die	6
SC	suprachiasmatic nucleus	Die	5,6	VMes	mesencephalic ventricle	Mes	6
SCO	subcommissural organ	Die	7-9	VOT	ventrolateral optic tract	Die	9-14
SD	saccus dorsalis	Die	3-6	Vp	postcommissural nucleus of the V	Tel	6-11
SGa	intermediate ganglionic layer	Rho	13-21	Vs	supracommissural nucleus of	Tel	4
SGr	granular layer	Rho	13-21		the V		3
SGT	secondary gustatory tract	Rho	16-27	VT	telencephalic ventricle	Tel	2-4
SMo	outer molecular layer	Rho	13-22	Vv	ventral nucleus of the V	Tel	2,3
SO	spinooccipital nerve						
SV	saccus vasculossus	Die	11-14	I	olfactory nerve		
SY	sulcus ypsiloniformis	Tel	3,4	II	optic nerve		
Tel	telencephalon			III	oculomotor nerve		
TeO	optic tectum	Mes	6-15	IV	trochlear nerve		
TL	torus longitudinalis	Mes	7-15	V	trigeminal nerve		
TPp	periventricular nucleus of the			VI	abducens nerve		
	posterior tuberculum	Die	7-10	VII	facial nerve		
TS	torus semicircularis	Mes	10-14	VIIs	sensory root of the facial nerve	Rho	17-23
TSc	central nucleus of the TS	Mes	11-14	VIII	octaval nerve		
TSvl	ventrolateral nucleus of the TS	Mes	11-14	IX	glossopharyngeal nerve		
TTB	tractus tectobulbaris	Mes	11-14	X	vagal nerve		

BRAIN ATLAS

The brain atlas of the eel is shown in Fig. 2. All descriptions refer the previous morphological reports from various fishes: the European eel (Meredith and Roberts, 1986, 1987; Meredith *et al*., 1987; Roberts *et al*., 1989; Wullimann *et al*., 1991; Molist *et al*., 1993), the rainbow trout (Meek & Nieuwenhuys, 1998), the gray mullet (Díaz-Regueira & Anadón, 1992), the goldfish (Peter & Gill, 1975; Morita & Finger, 1987a, b; Goehler & Finger, 1992), the zebrafish (Wullimann *et al*., 1996), the catfish (Kanwal & Caprio, 1987), or other teleosts (Meek & Nieuwenhuys, 1998). Basically, nomenclature of the nuclei and the fiber tracts corresponds to Wullimann *et al*. (1996) and Meek and Nieuwenhuys (1998), and is abbreviated as shown in Table 1.

Forebrain

The eel forebrain consisted of the olfactory bulb (OB) rostrally, the telencephalon (Tel) caudally, and the diencephalon (Die) ventrally. In the OB, three ring-like layers were observed (Plane 1), corresponding respectively to the internal cellular layer (ICL), the external cellular layer (ECL), and the glomerular layer (GL) in the zebrafish (Wullimann *et al*., 1996). Every layer consisted of small neurons (ca. 5 μm), and the density of the somata was highest in the GL.

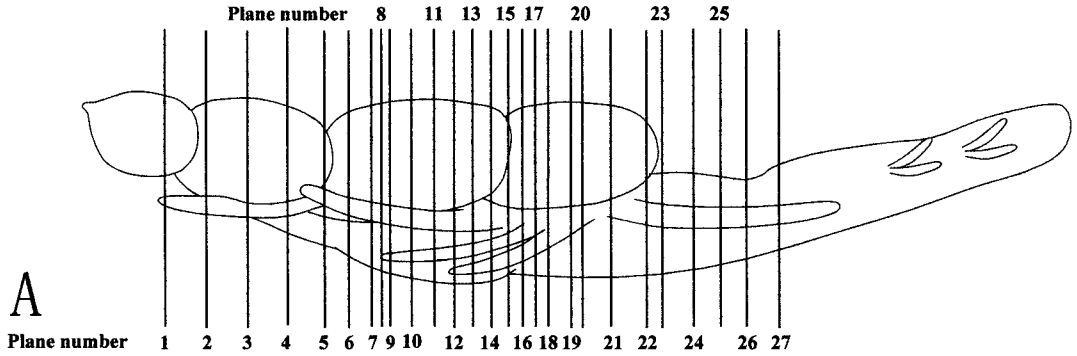

Fig. 2. Brain atlas of the Japanese eel (cross section). **A:** Lateral view of the eel brain indicating the levels (planes) for cross sectioning. Plane numbers (1-27) were given orderly from rostral to caudal. **B:** Cross section of the eel brain. Klüver-Barréra's staining is shown on the left and a schematic illustration of the figure is drawn on the right. Somata are colored violet and fibers blue. Blood vessels are omitted in the illustrations. Scale bar (200 μm) is common in all planes 1-27. The nuclei and the fiber trunks are all abbreviated as shown in Table 1.

Telencephalon. The telencephalon (Tel) was divided into the left and right telencephalic hemispheres by a central cavity, the telencephalic ventricle (VT). The telencephalic hemisphere consisted of the dorsal and ventral telencephalic areas. The dorsal telencephalic area (D) was composed of small granular somata (Planes 2, 3). At the middle part of the Tel, the D was subdivided into the central (Dc), the medial (Dm), the dorsal (Dd), and the lateral (Dl) zones (Plane 3). At the caudal part, the Dl was further subdivided into the dorsal (Dld) and the ventral (Dlv) parts by a hollow (Plane 4). A distinct concavity between the Dm and the Dd was identified as the sulcus ypsiloniformis (SY) (Planes 3, 4). The Dd was characterized as condensed somata (Plane 4). The ventral telencephalic area (V) was subdivided into five nuclei; the dorsal (Vd), the ventral (Vv), the lateral (Vl), the supracommissural (Vs) and the postcommissural (Vp) nuclei (Planes 2-4).

Fiber tracts. The medial olfactory tract (MOT) ran through the middle part of the Tel (Planes 2, 3), while the lateral olfactory tract (LOT) disappeared at the anterior part of the telencephalon (Planes 2, 3). The telencephalic hemispheres were connected with the anterior commissure (Cant) at the caudal part (Plane 4). In the caudal Tel, the median forebrain (MFB) and lateral forebrain (LFB) bundles were morphologically distinguished (Plane 4). Both bundles extended to the diencephalon (Die) (Planes 5, 6).

Diencephalon. The diencephalon (Die), located caudally to the Tel, was divided into six divisions; the preoptic area, the epithalamus, the thalamus, the hypothalamus, the posterior tuberculum and the pretectum. In the rostral part of the Die, the third ventricle (V3) appeared on the median line (Planes 4-9). At the caudal part, the V3 was expanded transversely and divided into the infundibulum (INF) (Planes 8-10) and the recess lateralis (RL) (Planes 9-11).

Preoptic area. The preoptic area surrounded the rostral part of the V3. The parvocellular preoptic nucleus (PP, < 5 μm) and the magnocellular preoptic nucleus (PM, *ca*. 20 μm) were arrayed along the rostral V3, the PP ventrally and the PM dorsally (Plane 5). The ventral margin of the V3 was surrounded by the suprachiasmatic nucleus (SC) (Planes 5, 6).

Epithalamus. The epithalamus consisted of the habenular nucleus (Ha), the saccus dorsalis (SD) and the epiphysis (E; pineal gland). The Ha surrounded the dorsal periventricular region of the V3, and was divided into

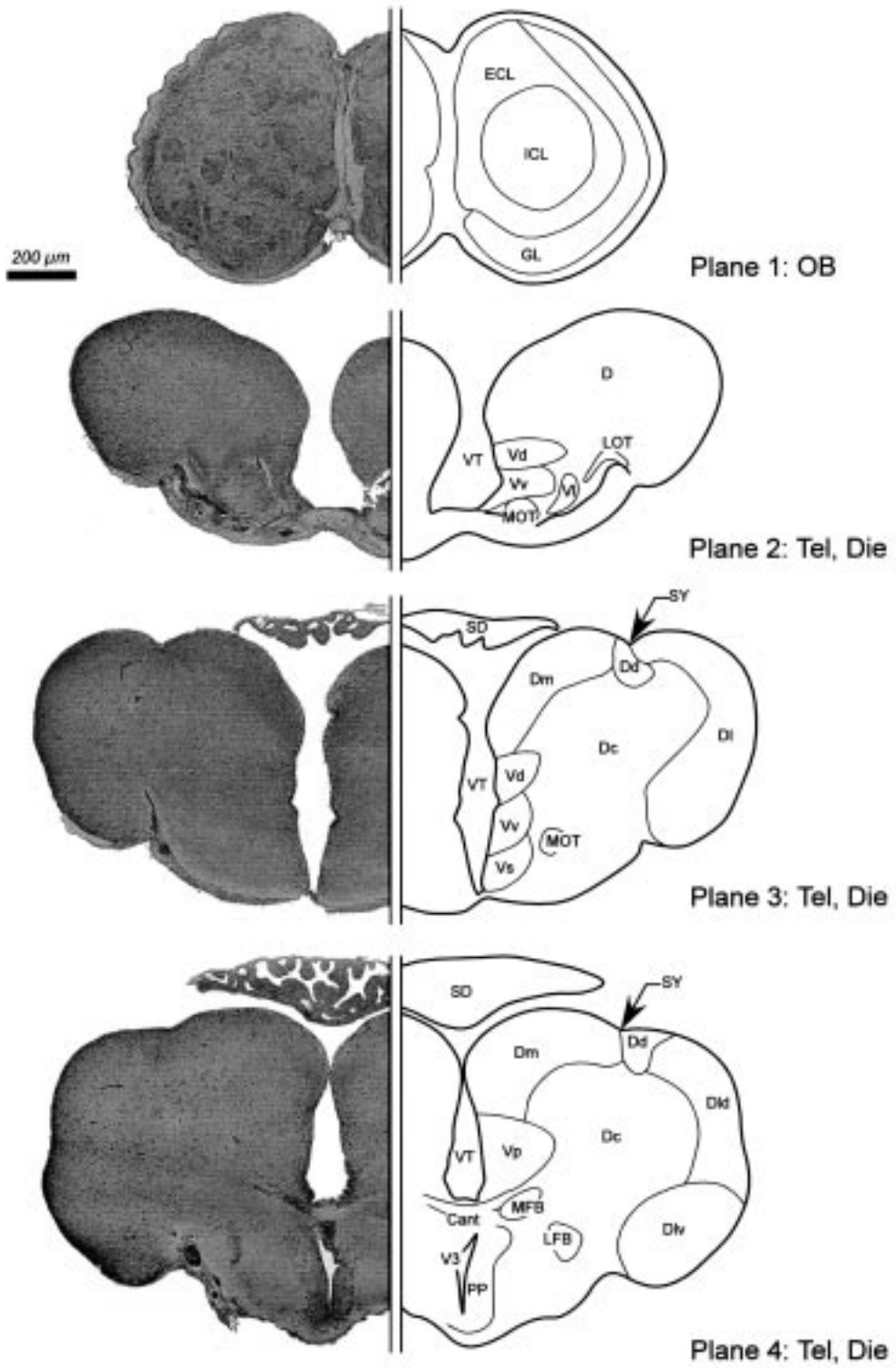
200 μm
ECL
ICL
GL
Plane 1: OB
D
VT
Vd
Vv
Vl
LOT
MOT
Plane 2: Tel, Die
SY
SD
Dm
Dd
Dl
Dc
VT
Vd
Vv
Vs
MOT
Plane 3: Tel, Die
SD
SY
Dm
Dd
Dld
Dc
VT
Vp
MFB
Cant
LFB
Dlv
V3
PP
Plane 4: Tel, Die

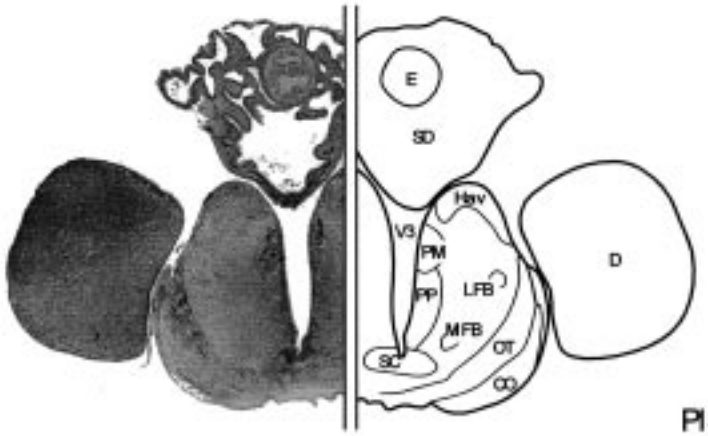

Plane 5: Die, Mes

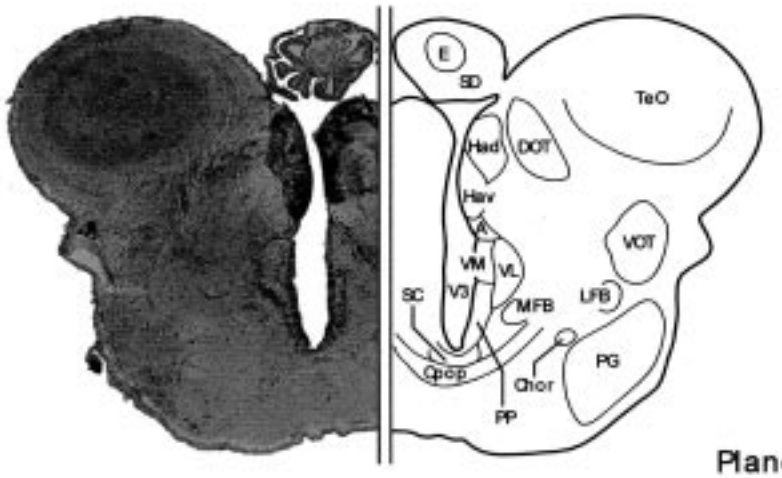

Plane 6: Die, Mes

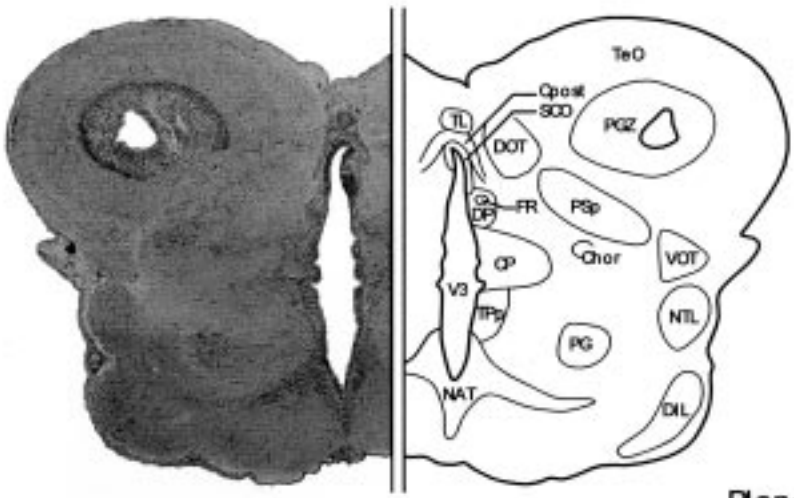

Plane 7: Die, Mes

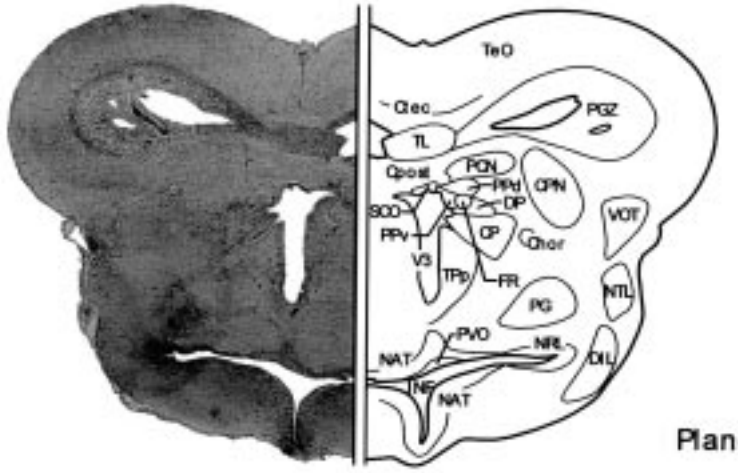

Plane 8: Die, Mes

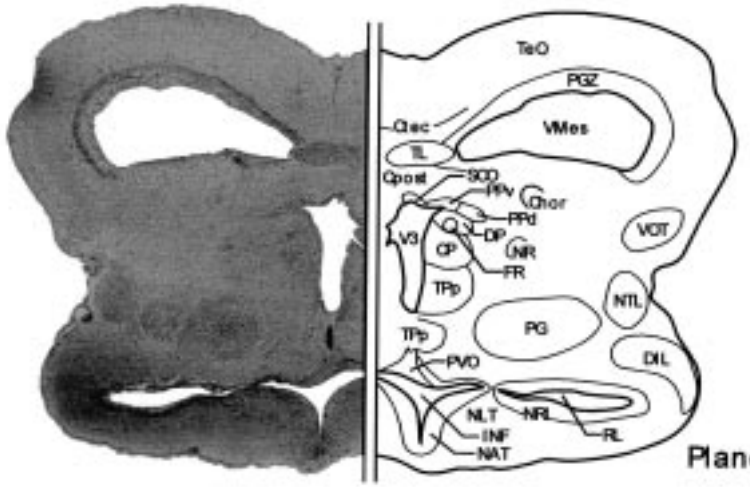

Plane 9: Die, Mes

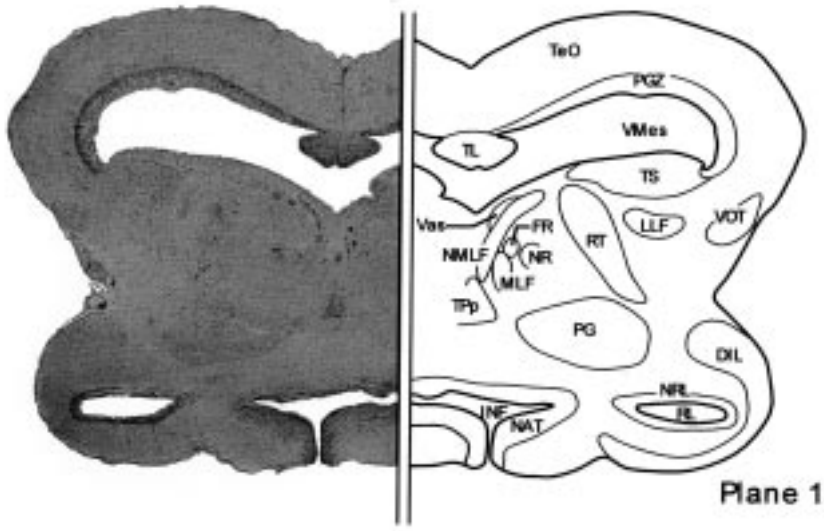

Plane 10: Die, Mes

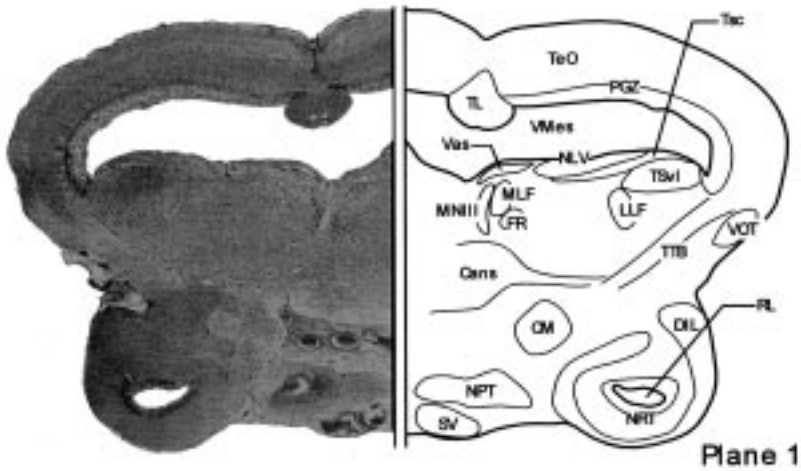

Plane 11: Die, Mes

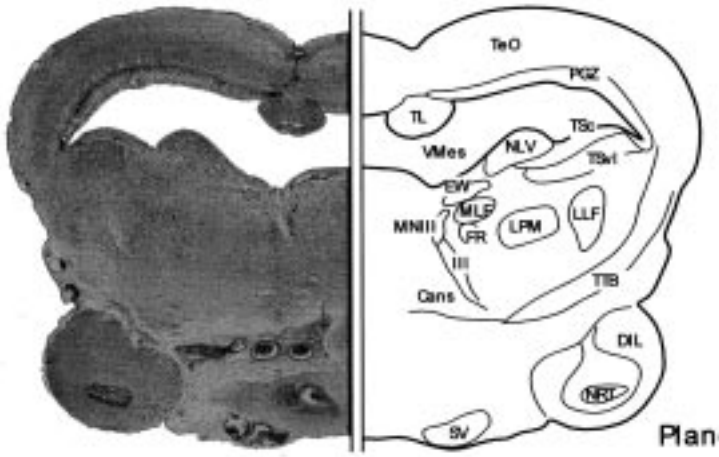

Plane 12: Die, Mes

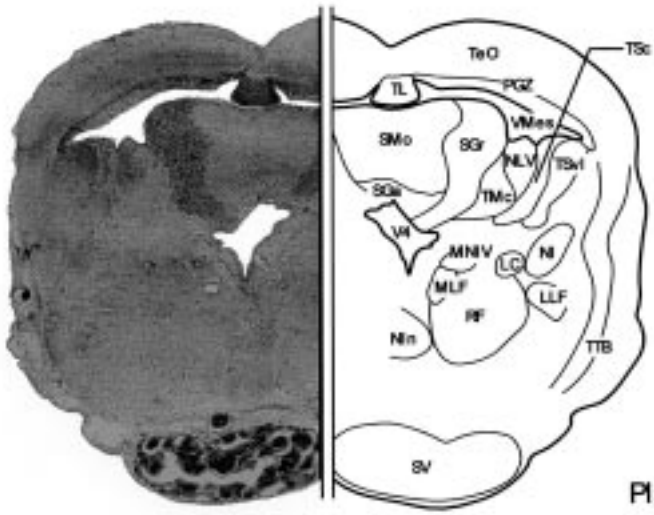

Plane 13: Die, Mes, Rho

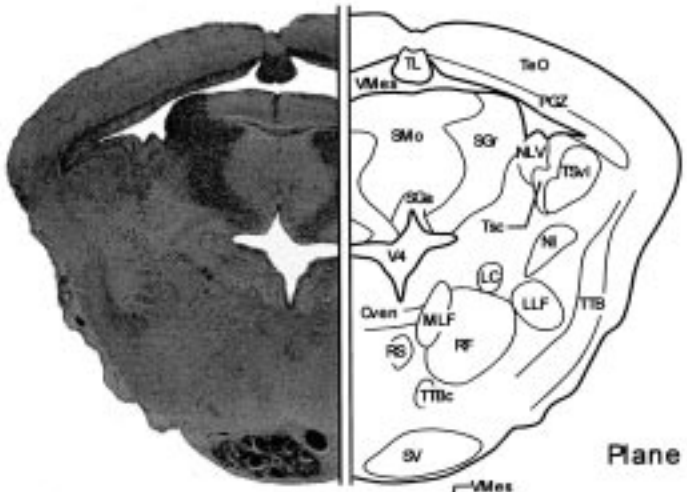

Plane 14: Die, Mes, Rho

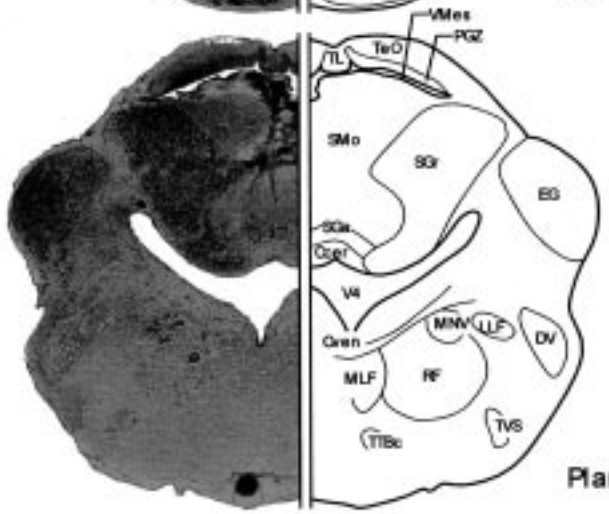

Plane 15: Mes, Rho

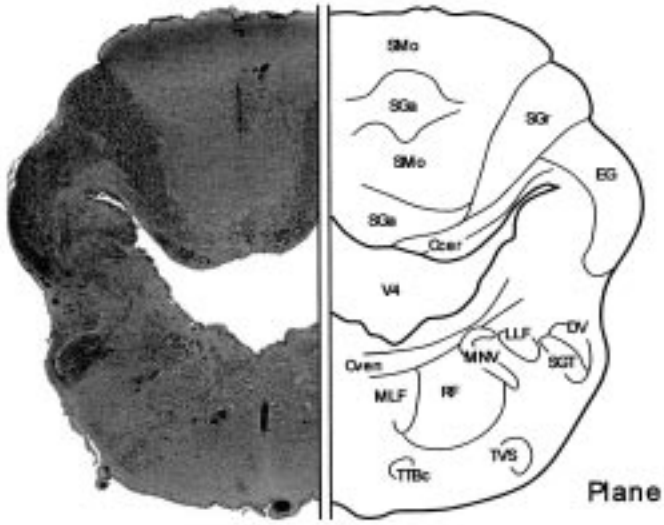

Plane 16: Rho

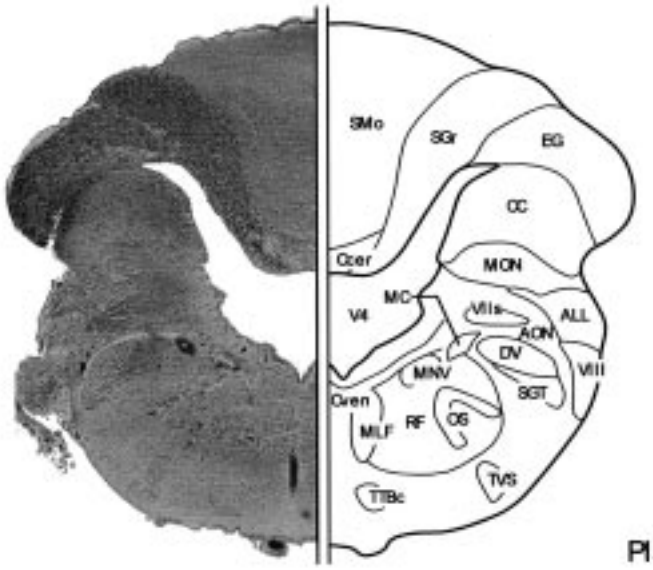

Plane 17: Rho

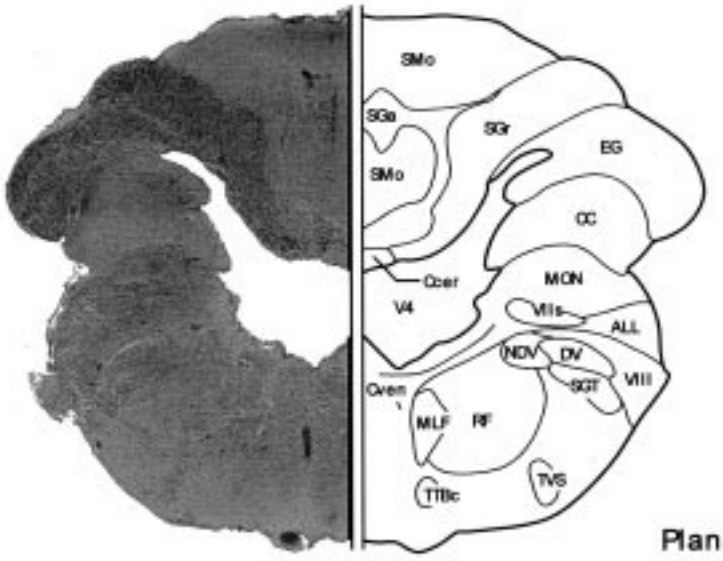

Plane 18: Rho

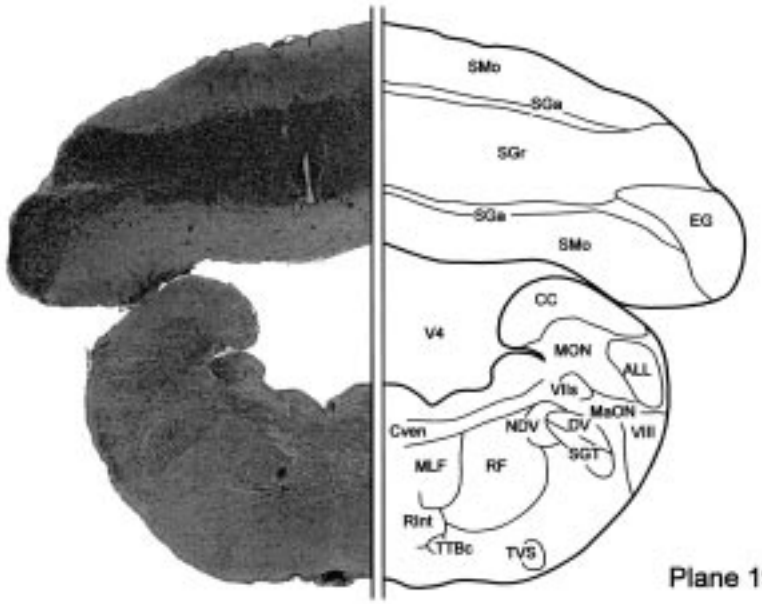

Plane 19: Rho

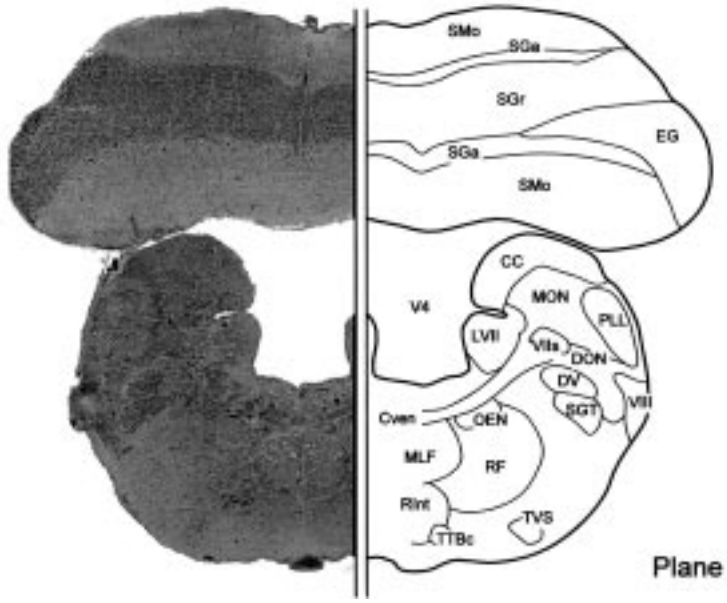

Plane 20: Rho

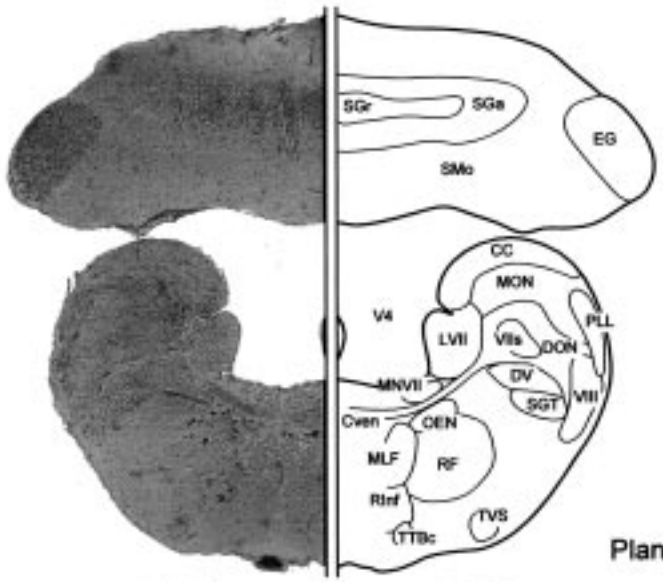

Plane 21: Rho

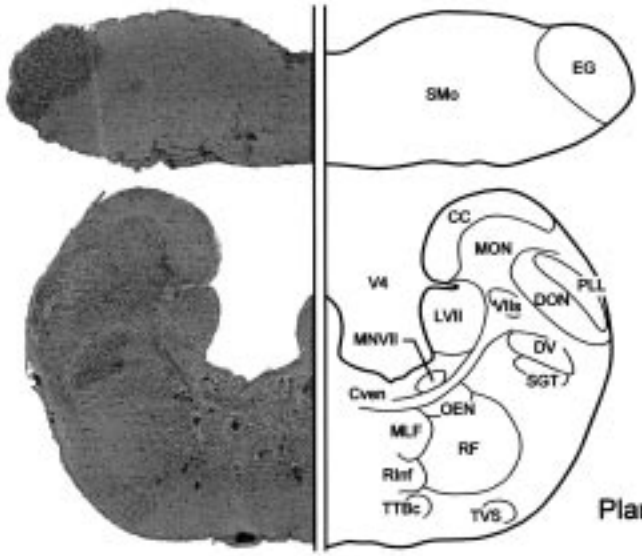

Plane 22: Rho

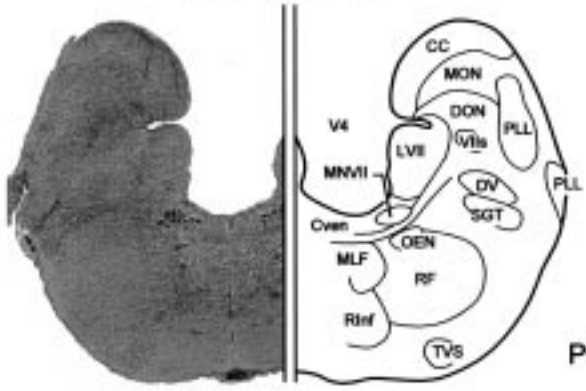

Plane 23: Rho

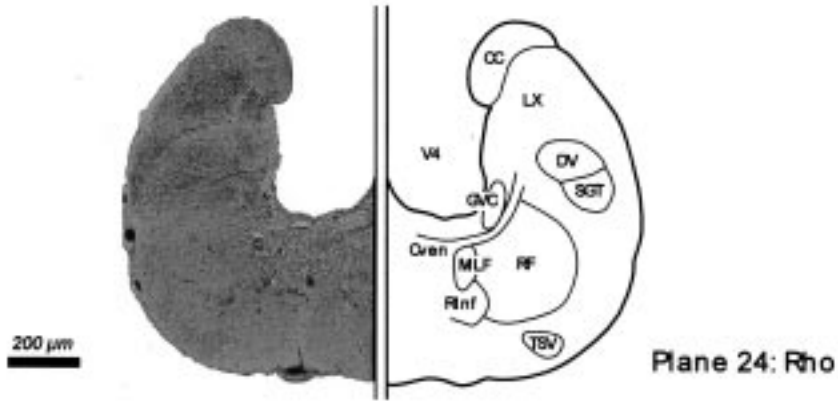

Plane 24: Rho

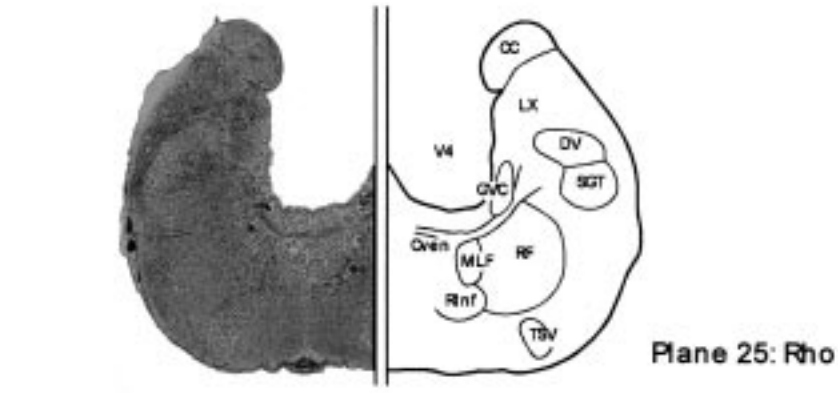

Plane 25: Rho

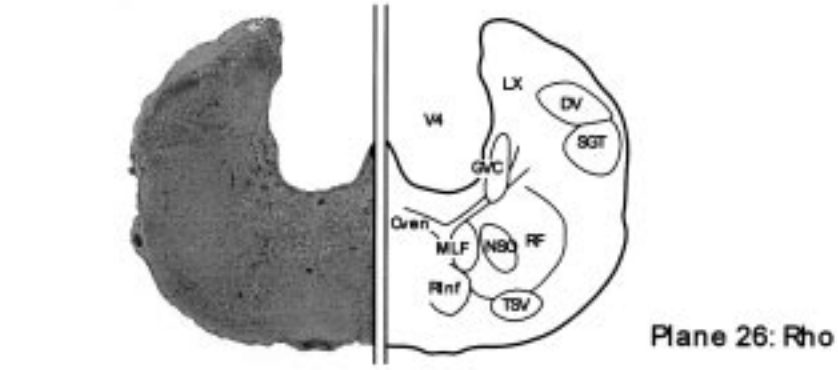

Plane 26: Rho

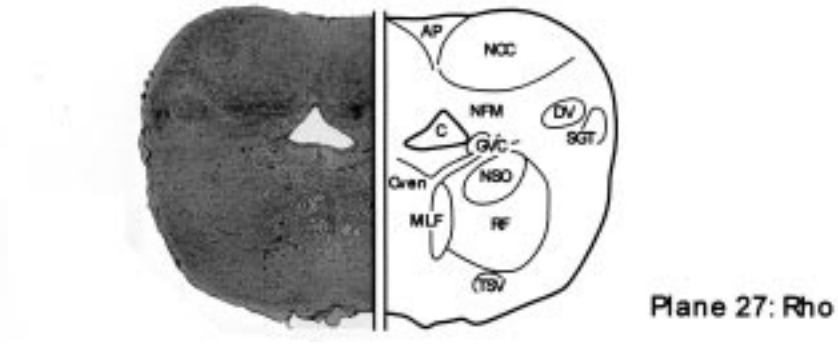

Plane 27: Rho

two parts by a staining pattern; the dorsal (Had) and the ventral (Hav) habenular nuclei (Planes 5, 6). The SD projected rostrally and covered the telencephalic ventricle (VT) and the V3 (Planes 2-6).

Thalamus. The thalamus was located caudally to the epithalamus, and characterized by five nuclei; the anterior, the dorsal posterior, the central posterior, the ventromedial, and the ventrolateral thalamic nuclei. The anterior thalamic nucleus (A) was located beneath the ventral habenular nucleus (Hav) (Plane 6). Further ventrally, the ventromedial (VM) and the ventrolateral (VL) thalamic nuclei were situated (Plane 6). Caudally to the A, the dorsal posterior thalamic nucleus (DP) and the central posterior thalamic nucleus (CP) appeared along the V3 (Planes 7-9).

Posterior tuberculum. The posterior tuberculum (TP) was located caudally to the ventral thalamus, and elongated caudally along the V3. The rostralmost part of the TP was the periventricular nucleus of the posterior tuberculum (TPp) (Planes 7-10). Ventrally to the TPp, the paraventricular organ (PVO) appeared abut on the infundibulum (INF) (Planes 8, 9). The PVO was characterized by well-developed vasalia. Laterally to the TPp, there were the preglomerular nucleus (PG) centrally (Planes 7-10), and the nucleus tori lateralis (NTL) more peripherally (Planes 7-9). At the caudalmost part of the TP, there was the corpus mamillare (CM) centrally (Plane 11).

Hypothalamus. In the hypothalamus, the infundibulum (INF) appeared ventrally to the V3 (plane 8), and the INF was further expanded laterally to form the recess lateralis (RL) at more caudal part (Plane 9-11). Most hypothalamic nuclei were situated along these ventricles. At the rostralmost part, the anterior tuberal nucleus (NAT) appeared beneath the V3 (Plane 7) and the NAT surrounded the INF (Planes 8-10), which was surrounded by the posterior tuberal nucleus (NPT) at the more caudal part (Plane 11). Around the RL, the nucleus recessi lateralis (NRL) existed periventricularly (Planes 8-12). Peripherally in the inferior lobe (IL), the diffuse nucleus of the inferior lobe (DIL) was observed (Planes 7-12). The saccus vasculosus (SV) appeared at the ventromedian area of the hypothalamus, caudally to the pituitary (Planes 11-14).

Pretectum. The pretectal region between the diencepharon (Die) and the mesencephalon (Mes) was characterized by the relatively thick posterior commissure (Cpost) situated above the V3 (Planes 7-9). Beneath the Cpost, the subcommissural organ (SCO), consisting of well-developed ependymal cells, contacted with the V3 (Planes 7-9). Laterally to the SCO, the ventral and the dorsal parts of the periventricular pretectal nuclei (PPv and PPd) were distinguished (Planes 8, 9). Dorsally to the PPd, the paracommissural nucleus (PCN) was detected and the central pretectal nucleus (CPN) was distingished laterally to the PCN (Plane 8). At more rostral part, the parvocellular superficial pretectal nucleus (PSp) was observed (Plane 7).

Fiber tracts. In the ventrolateral side of the Die, the optic tract (OT) and the optic chiasm (CO) extended ventrolaterally (Plane 5). The postoptic commissure (Cpop) appeared caudally to the optic chiasm (CO) (Plane 6). The dorsomedial optic tract (DOT) extended dorsally toward the optic tectum (TeO) (Planes 6, 7), while the ventrolateral optic tract (VOT) was elongated more caudally (Planes 6-11). The fasciculus retroflexus (FR) emerged caudally to the habenular nucleus (Ha) in the epithalamus (Plane 7) and extended to a region of the mesencephalon (Mes), where the interpeduncular nucleus (NIn) appeared (Plane 13). The horizontal commissure (Chor) emerged ventrally in the rostral Die (Plane 6), went up to the dorsal side, and then ran longitudinally to the mesencephalic region (Planes 7-9).

Midbrain (Mesencephalon)

The mesencephalon (Mes) was characterized by the dorsally expanded optic tectum (TeO) and the wide

mesencephalic ventricle (VMes) (Planes 7-15), and was divided into three major divisions from dorsal to ventral; the optic tectum, the torus semicircularis and the tegmentum.

Optic tectum. The somata of the TeO were condensed as a layer along the VMes (Planes 6-15), forming the periventricular gray zone (PGZ) of the TeO. The torus longitudinalis (TL) hung over the median VMes and extended rostrocaudally (Planes 7-15). Above the TL, the commissura tecti (Ctec) connected both lobes of the TeO (Planes 8, 9).

Torus semicircularis. The torus semicircularis (TS), situated ventrolaterally to the VMes and consisted of many condensed somata, was expanded into the VMes (Planes 10-14). The TS was subdivided into the ventrolateral nucleus of the torus semicircularis (TSvl) and the central nucleus of the torus semicircularis (TSc) (Planes 11-14).

Tegmentum. The tegmentum, ventromedian region to the TS, possessed large somata (> 20 μm). The somata of the nucleus ruber (NR), located in the rostralmost part of the tegmentum, were oval in shape (*ca*. 25 μm) (Planes 9, 10). In the more median side of the NR, there was the nucleus of the medial longitudinal fascicle (NMLF) (Plane 10). The cell bodies of the NMLF were oval or round in shape with huge size (*ca*. 40 μm). In the rostral tegmentum, the vascular lacuna of area postrema (Vas) occurred as a well-developed vasalium in the median corner facing to the VMes (Planes 10, 11). Laterally to the NMLF, the rostral tegmental nucleus (RT) was identified as a dorsoventrally diffused cluster (Plane 10). Caudally to the NMLF, many medium-sized (*ca*. 10 μm) and oval perikarya were conspicuously distinguished around the median line (Planes 11-13). These somata were classified into three groups: the oculomotor nucleus (MNIII) (Planes 11, 12), the Edinger-Westphal nucleus (EW) (Plane 12) and the trochlear nucleus (MNIV) (Plane 13). The nucleus lateralis valvulae (NLV) was protruded to the VMes (Planes 11, 12). The protruded region of the NLV extended caudally, and then fused with the valvula cerebelli in the rhombencephalon (Rho) (Planes 13, 14). Ventrally to the NLV, the nucleus lateralis profundus mesencephali (LPM) was distinguished (Plane 12). In the caudal part of the tegmentum, the interpeduncular nucleus (NIn) was present at the median portion (Plane 13).

Fiber tracts. Two major longitudinal bundles were distinguished in the midbrain; the medial longitudinal fascicle (MLF) (Planes 10-27) and the lateral longitudinal fascicle (LLF) (Planes 10-16). The MLF started near the NMLF, while the LLF started beneath the torus semicircularis (TS) (Plane 10). Both fascicles extended caudally toward the rhombencephalon (Rho). The tractus tectobulbaris (TTB) traversed from the TeO to the ventro-median part of the tegmentum (Planes 11-14). Many fibers of the TTB crossed the median line through the ansulate commissure (Cans) (Planes 11, 12), which was located rostrally to the NIn (Plane 13). Beneath the MNIII, the oculomotor nerve (III) extended to the ventral region (Plane 12).

Hindbrain (Rhombencephalon)

The rhombencephalon (Rho), the most caudal brain (hindbrain), consisted of the metencephalon and the myelencephalon. Since fish lack the pons, the metencephalon means the cerebellum (Ce), and the myelencephalon is the medulla oblongata (MO).

Cerebellum. The cerebellum (Ce) was divided into three main regions longitudinally; the valvula cerebelli, the corpus cerebelli, and the caudal cerebellar region. The valvula cerebelli represented a median bulge into the VMes, and consisted of three layers; the outer molecular layer (SMo), the intermediate ganglionic layer (SGa), and the deep granular layer (SGr) (Planes 13-15). The corpus cerebelli was also composed of three major layers of the SMo, the SGa and the SGr (Planes 16-22). The size (ca. 5 μm) and distribution of the SGa neurons in the

eel was relative to those of Purkinje cells in the rainbow trout (Meek & Nieuwenhuys, 1998). The granular eminence (EG) emerged at the junction between the Ce and the MO (Plane 15) and ran caudally (Planes 15-22). The caudal cerebellar region was turned rostrally and connected to the MO by the crista cerebellaris (CC) (Planes 17-25). At the ventral part of the Ce, the cerebellar commissure (Ccer) was distinguished above the fourth ventricle (V4) (Planes 15-18).

Fourth ventricle. Between the cerebellum (Ce) and the medulla oblongata (MO), there existed the huge ventricle, fourth ventricle (V4). However, the V4 was extremely narrow at the rostral part (Plane 13, 14). It became wider caudally (Plane 15-18) with greatest width at the middle part of the MO (Plane 17, 18), and then the width was reduced gradually (Plane 19-26).

Medulla oblongata. The medulla oblongata (MO) was connected with the mesencephalon at the rhombencephalic isthmal region rostrally (Plane 13) and with the spinal cord at the obex (OX) level caudally (Plane 27).

Rostral area (planes 13-17). In the rostralmost part of the MO, the nucleus isthmi (NI) was located mid-laterally (Planes 13, 14). At more median site of the NI, the locus coeruleus (LC) with several large-sized perikarya (*ca*. 20μm) and the superior raphe nucleus (RS), the most anterior part of the raphe nuclei on the medial line, were identified (Planes 13, 14). Caudally to the LC, the trigeminal motor nucleus (MNV) appeared (Planes 15-18). At more caudal part, the superior olive (OS) was located ventrally to the MNV (Plane 17). At the ventral part of the anterior octaval nucleus (AON), paired extremely huge perikarya were present (Plane 17). These perikarya were dorsolaterally elongated and ellipsoidal in shape (*ca*. 90 μm longitudinally and 50 μm transversely), and identified as the Mauthner cells (MC) following the observations in the European eel (Meredith and Roberts, 1987; Meredith *et al*., 1987), the goldfish (Nieuwenhuys *et al*., 1998), and various teleosts (Zottoli, 1978).

Middle area (Planes 17-23). At the middle part of the MO, the medial octavolateral nucleus (MON) emerged from the crista cerebellaris (CC) (Plane 17). The cell mass situated ventrally to the MON was divided rostrocaudally into three groups; the anterior octaval nucleus (AON) (Plane 17), the magnocellular octaval nucleus (MaON) (Plane 19) and the descending octaval nucleus (DON) (Planes 20-23). More caudally, the intermediate raphe nucleus (RInt) (Planes 19-20), the octavolateral efferent nucleus (OEN) (Planes 20-23), the facial motor nucleus (MNVII) (Planes 21-23), and the inferior raphe nucleus (RInf) (Planes 21-26) appeared. The lateral wall of the V4 was divided into the crista cerebellaris (CC) and the facial lobe (LVII) by a sulcus (Plane 20-23).

Caudal area (Planes 24-27). The glossopharyngeal (MNIX) and the vagal (MNX) motor nuclei were arrayed along the V4 as a continuous column (Planes 24-27), therefore the column was called glossopharyngeal-vagal motor complex (GVC). Ventrally to the GVC, the spinooccipital motor nucleus (NSO) consisting of multipolar or ellipsoidal medium-sized perikarya (*ca*. 20 μm) extended caudally beyond the obex (Planes 26, 27). The vagal lobe (LX) appeared caudally to the facial lobe (LVII) (Plane 24-26). At the most caudal area of the brain, the area postrema (AP) was recognized as a median structure with many capillaries in its dorsal region (Plane 27). Ventrolaterally to the AP, the commissural nucleus of the Cajal (NCC) and medial funicular nucleus (NFM) were distinguished (Plane 27). Both nuclei consisted of small diffuse somata.

Fiber tracts. The medial longitudinal fascicle (MLF) and the lateral longitudinal fascicle (LLF) were major longitudinal fascicles in the MO. The MLF extended caudally through the obex (OX) level (Planes 10-27), while the LLF disappeared at the anterior MO (Plane 17). In the octavolateral area, three fiber tracts were

distinguished; the anterior lateral line nerve (ALL) (Planes 17-19), the posterior lateral line nerve (PLL) (Planes 20-23) and the octaval nerve (VIII) (Planes 17-21). The tractus tectobulbaris cruciatus (TTBc) ran longitudinally in planes 15-23. The descending trigeminal root (DV) and the secondary gustatory tract (SGT) emerged at the Mes (Plane 15) and extended caudally through the OX (Plane 27). The vestibulo-spinal tract (TVS) emerged at the Mes (Plane 15) and elongated caudally through the OX (Plane 27) in parallel to the reticular formation (RF). The commissure ventralis rhombencephali (Cven) ran beneath the V4 or the central canal (C) (Planes 14-27).

Longitudinal distribution of medullary nuclei

Many nuclei in the MO were distributed longitudinally along the V4, mostly with a column structure, and some were already described above. The raphe nuclei were located in the median region of the MO, and consisted of three parts; the superior raphe nucleus (RS), the intermediate raphe nucleus (RInt), and the inferior raphe nucleus (RInf). The RS emerged immediately caudal to the NIn (Plane 14). Another two nuclei appeared below the medial longitudinal fascicle (MLF) (Planes 19, 20). The most caudal raphe nucleus was the RInf (Planes 21-26) (Fig. 3). Lateral to the raphe nuclei and the MLF, the reticular formation (RF) ran through the MO. Within the RF, there were large-sized somata (> 25 μm) with multipolar or oval shapes (Planes 13-27).

Figure 3 shows a schematic distribution of some major nuclei in the MO. The length of the column of the MNV, the MNVII and the GVC were approximately 450 μm, 500 μm, and 1700 μm, respectively. The gaps

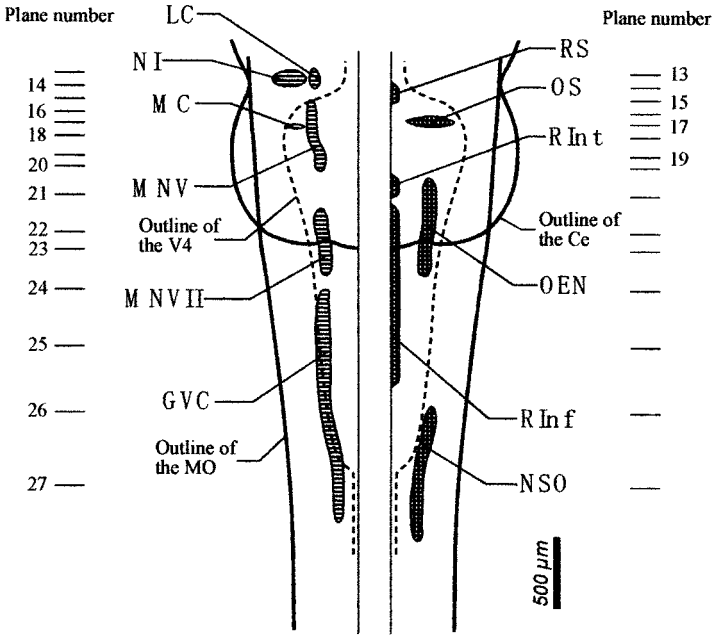

Fig. 3. Longitudinal distribution of various nuclei in the medulla oblongata (MO) (dorsal view). The figure is constructed schematically from the data of planes 13-27 in Fig. 2B. The left half nuclei situate dorsally to the right half nuclei. All abbreviations are illustrated in Table 1.

between the MNV and the MNVII and between the MNVII and the GVC were approximately 300 μm and 50 μm, respectively (left half in Fig. 3). The raphe nuclei (the RS, the RInt and the RInf) were arrayed on the median line, while the superior olive (OS), the octavolateral efferent nucleus (OEN) and the spinooccipital motor nucleus (NSO) were situated bilaterally (right half in Fig. 3). Therefore, the OEN and the NSO were positioned closely to the MNVII and the GVC (Planes 21-23) (Planes 26, 27), and the formers (left half in Fig. 3) were ventral to the latter (right half in Fig. 3).

Cranial ganglia. Apart from the brain, three ganglia of the trigeminal nerve (V), the facial nerve (VII), and the glossopharyngeal (IX) or the vagal (X) nerve were observed at the level of planes 13-15, of planes 15-16, and of planes 19-26, respectively (data not shown). The somata in these ganglia are all round-shaped (> 20 μm). These ganglia may correspond to the semilunar, geniculate, and jugular/nodose ganglia in human, respectively (Martini *et al*., 2000).

DISCUSSION

The external morphology of the eel brain was characterized by a close apposition between the olfactory bulb (OB) and the telencephalon (Tel), a relatively small expansion of the optic tectum (TeO), a smooth boundary between the medulla oblongata (MO) and the spinal cord, and three lobes of the cerebellum (Ce). A similar juxtaposition of the OB and Tel is also observed in the zebrafish (Wullimann *et al*., 1996) and the rainbow trout (Nieuwenhuys *et al*., 1998), while the OB is separated from the Tel in the goldfish (Morita and Finger, 1987a; Nieuwenhuys *et al*., 1998). The TeO covers the midbrain dorsolaterally in the eel, while ventrolaterally in the rainbow trout (Nieuwenhuys *et al*., 1998), the zebrafish (Wullimann *et al*., 1996), and the goldfish (Morita and Finger, 1987a; Nieuwenhuys *et al*., 1998). The eel medulla oblongata (MO) shifts gradually to the spinal cord as in the rainbow trout (Nieuwenhuys *et al*., 1998), while the caudal part of the MO expands dorsally to form the facial (LVII) and vagal (LX) lobes in the zebrafish (Wullimann *et al*., 1996) and the goldfish (Nieuwenhuys *et al*., 1998). The fourth ventricle (V4) of the eel seems to be longer than those of the zebrafish (Wullimann *et al*., 1996) and the goldfish (Nieuwenhuys *et al*., 1998), whose V4 are covered with the LVII. In the rainbow trout, the V4 is completely covered with the Ce, and thus not visible from the outside.

The present study is the first report of the whole brain atlas of the eel, whereas partial brain morphology has been described in the European eel (Meredith and Roberts, 1986, 1987; Meredith *et al*., 1987; Roberts *et al*., 1989; Wullimann *et al*., 1991; Molist *et al*., 1993), and all results obtained in this study are consistent with the restricted descriptions in the European eel. Figures 4 and 5 summarize the brain nuclei and the fiber tracts identified in the present study, respectively. A hierarchical representation of the anatomical nomenclature serves to establish the relationship among structures and provides a map of the organization of the nervous system. Many nuclei in Fig. 4 appear to be adjacent to the ventricles in general.

Basically, the brain topology of the eel is similar to those of the rainbow trout (Meek and Nieuwenhuys, 1998), the goldfish (Peter and Gill, 1975; Morita and Finger, 1987a, b; Goehler and Finger, 1992; Meek and Nieuwenhuys, 1998), the zebrafish (Wullimann *et al*., 1996), and the catfish (Kanwal and Caprio, 1987). However, some fine structures differ from those of other teleosts. 1) The parvocellular preoptic nucleus (PP) could not be subdivided in the eel, whereas the anterior and posterior parts of the PP are distinguished in the zebrafish (Wullimann *et al*., 1996) and the rainbow trout (Meek and Nieuwenhuys, 1998). 2) The intermediate thalamic nucleus was not distinguished in the eel thalamus, although it is located dorsally to the ventromedial and vent-

rolateral thalamic nuclei (VM and VL) in the zebrafish (Wullimann *et al*., 1996), the goldfish (Nieuwenhuys *et al*., 1998), and the rainbow trout (Nieuwenhuys *et al*., 1998). The ventral thalamic nuclei are known to have a different distribution among teleosts (Wullimann *et al*., 1991). 3) The paraventricular organ (PVO) was single in the eel, while paired PVOs are observed in the zebrafish (Wullimann *et al*., 1996). 4) The torus semicircularis (TS) in the eel was smaller than that in the goldfish (Peter and Gill, 1975) and rainbow trout (Nieuwenhuys *et al*., 1998). 5) The cell size (40 μm) of the nucleus of medial longitudinal fascicle (NMLF) in the tegmentum was similar to that in the elephantfish (Hlavacek *et al*., 1984), but larger than that in the glass knifefish (Behred and Donicht, 1990), or the zebrafish (Wullimann *et al*., 1996). 6) The protrusion of the nucleus lateralis valvulae (NLV) into the mesencephalic ventricle (VMes) in the eel was larger than that in the zebrafish (Wullimann *et al*., 1996) and the rainbow trout (Nieuwenhuys *et al*., 1998). 7) The valvula cerebelli in the eel was similar to that in the rainbow trout (Nieuwenhuys *et al*., 1998), but smaller than those in the goldfish (Peter and Gill, 1975) and the zebrafish (Wullimann *et al*., 1996). 8) The facial lobes (LVII) ran through the medulla oblongata (MO) in the eel similarly as in the rainbow trout (Nieuwenhuys *et al*., 1998), while two lobes fuse at the caudal cerebellum in the goldfish (Morita and Finger, 1987a; Nieuwenhuys *et al*., 1998), the catfish (Kanwal and Caprio, 1987; Nieuwenhuys *et al*., 1998), and the zebrafish (Wullimann *et al*., 1996). 9) The expansion of the vagal lobe (LX) in the caudal MO of the eel was similar to that in the gray mullet (Diaz-Regueira and Anadón, 1992) and the rainbow trout (Nieuwenhuys *et al*., 1998), but smaller than that in the goldfish (Morita and Finger, 1987a, b; Goehler and Finger, 1992) and the zebrafish (Wullimann *et al*., 1996). 10) The glossopharyngeal motor nucleus (MNIX) and the vagal motor nucleus (MNX) were fused to make a columnar structure named glossopharyngeal-vagal motor complex (GVC). Similar complex is observed in the lamprey (Aríëns-Kappers *et al*., 1936), the elasmobranch (Aríëns-Kappers *et al*., 1936; Anadón *et al*., 2000) and other teleost fishes (Aríëns-Kappers *et al*., 1936; Kanwal and Caprio, 1987; Morita and Finger, 1987b; Goehler and Finger, 1992; Wullimann *et al*., 1996; Nieuwenhuys *et al*., 1998; Pérez *et al*., 2000). Therefore, such a columnar complex seems to be common in fishes. 11) The facial motor nucleus (MNVII) was separated from the GVC in the eel similarly as in the bowfin (Nieuwenhuys *et al*., 1998), the catfish (Kanwal and Caprio, 1987), the rainbow trout (Pérez *et al*., 2000), the anglerfish (Aríëns-Kappers *et al*., 1936), the puffer fish (Aríëns-Kappers *et al*., 1936), the sunfish (Aríëns-Kappers *et al*., 1936), and the goldfish (Morita and Finger, 1987b; Goehler and Finger, 1992; Nieuwenhuys *et al*., 1998), whereas it is fused with the GVC in the sturgeon (Adrio *et al*., 2000), the reedfish (Aríëns-Kappers *et al*., 1936) and the tarpon (Aríëns-Kappers *et al*., 1936).

Among the nuclei identified in the present study, the magnocellular preoptic nucleus (PM), anterior tuberal nucleus (NAT), area postrema (AP), and glossopharyngeal- vagal motor complex (GVC) might be involved in drinking behavior in the Japanese eel. The PM, the NAT and the AP seem to be the circumventricular organs which lack the blood-brain barrier (BBB) and thus accept dipsogens and antidipsogens produced in the systemic circulation, because these nuclei are stained by intraperitoneal Evans blue which can not pass the BBB (T. Mukuda, Y. Matsunaga, K. Kawamoto, K. Yamaguchi and M. Ando, unpublished observation). The GVC innervates the upper esophageal sphincter muscle cholinergically (Mukuda and Ando, 2003; Kozaka and Ando, 2003).

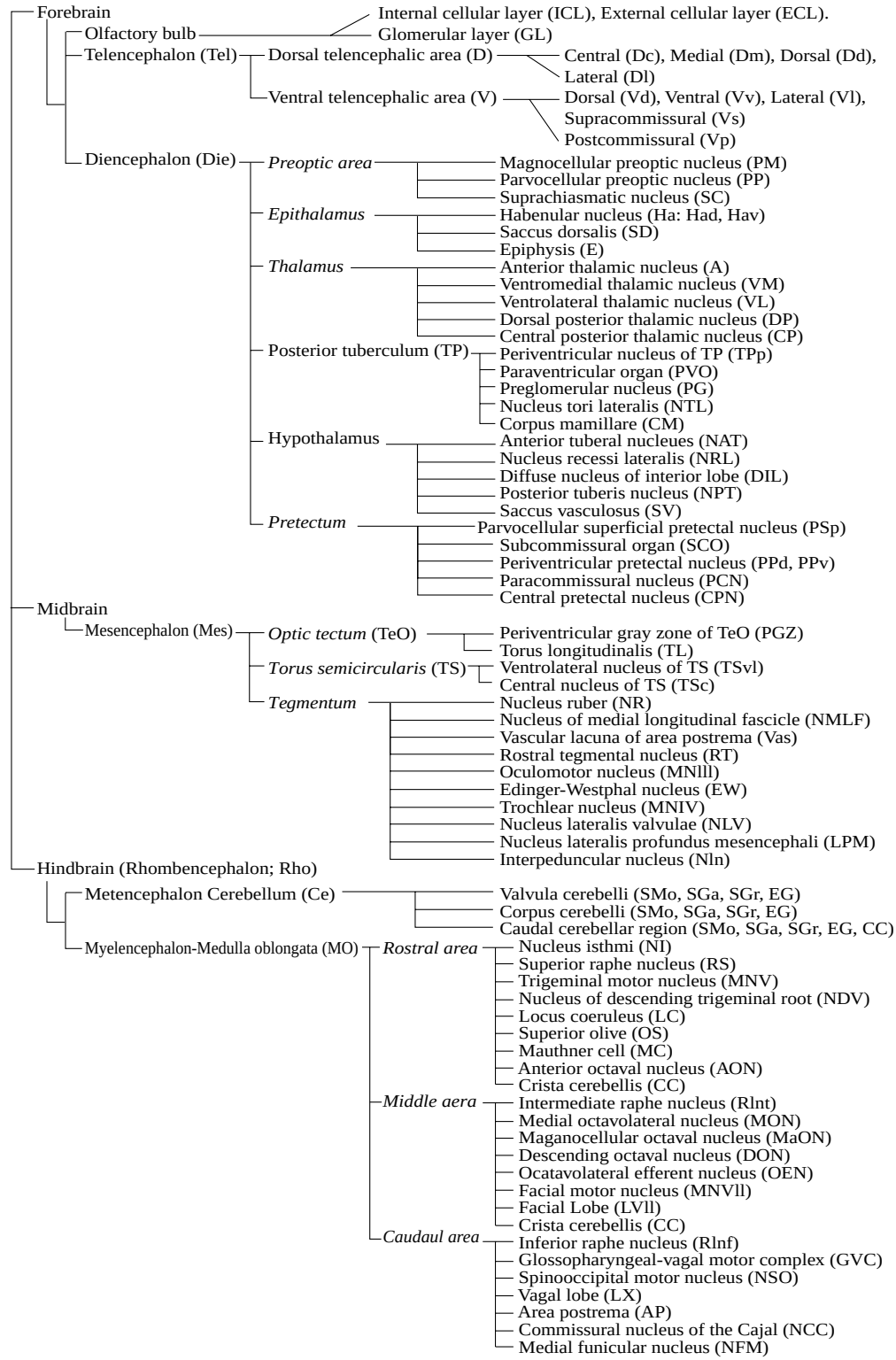

Fig. 4. Brain tree of the Japanese eel. Brain nuclei identified in the present study are classified to three regions, and further subdivided following the book by Toga and Mazziotta (1996).

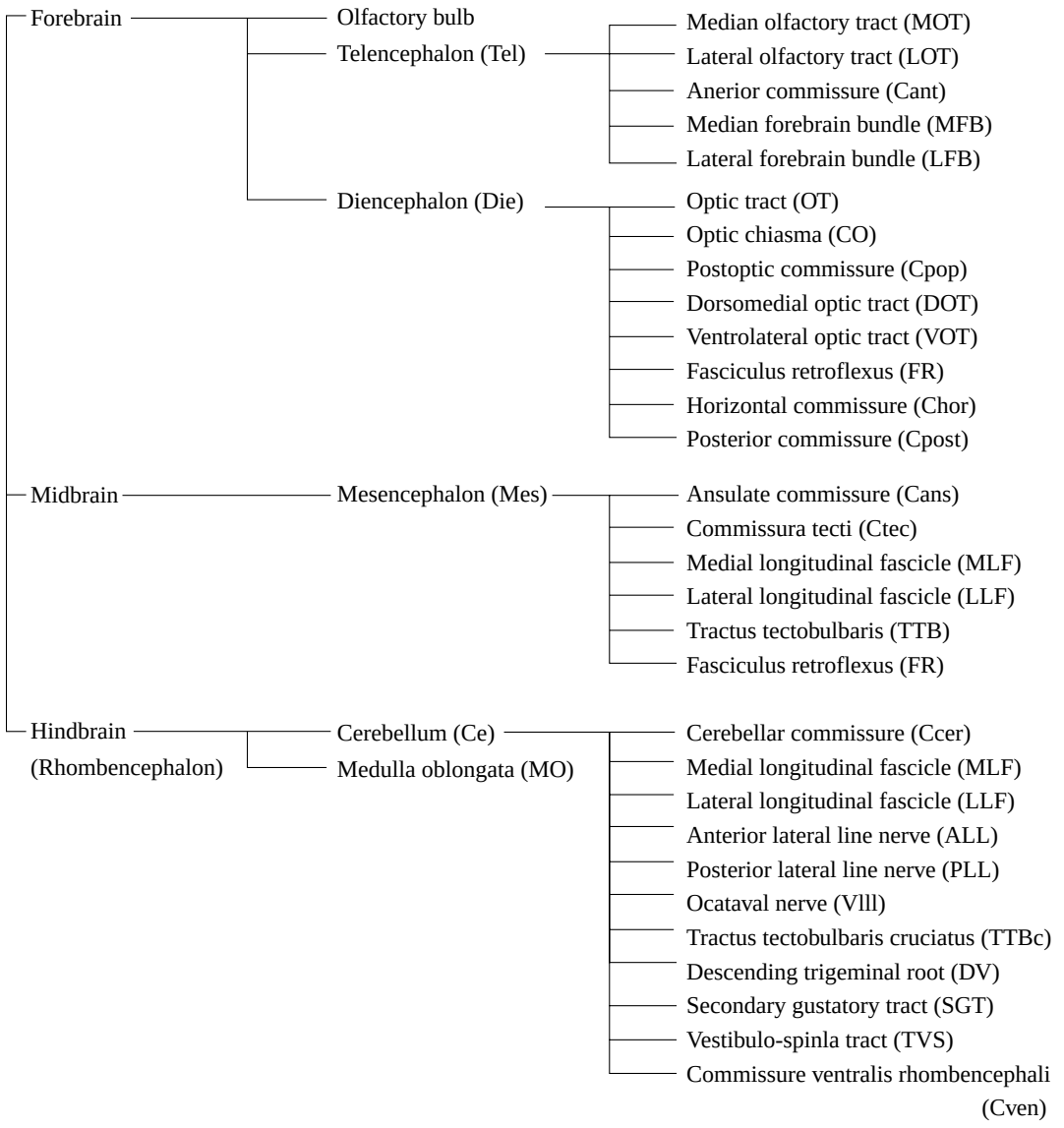

Fig. 5. Fiber tracts in the brain of the Japanese eel. Fiber tracts identified in the present study are classified following the anatomical distribution.

ACKNOWLEDGMENTS

This research was supported in part by Grants-in-Aid for Scientific Research (C) nos.13640681 and 15570064 from the Ministry of Education, Culture, Sports, Science and Technology, Japan, and also by the Fisheries Agency of Japan.

References

Adrio F, Anadón R Rodriguez-Moldes I (2000) Distribution of choline acetyltransferase (ChAT) immunoreactivity in the central nervous system of a chondrostean, the Siberian sturgeon (*Acipenser baeri*). J Comp Neurol 426: 602-621

Anadón R, Molist R, Rodriguez-Moldes I, Lopez JM, Quintela I, Cervino MC, Barja P, Gonzalez A (2000) Distribution of choline acetyltransferase immunoreactivity in the brain of an elasmobranch, the lesser spotted dogfish (*Scyliorhinus canicula*). J Comp Neurol 420: 139-170

Ando M, Fujii Y, Kadota T, Kozaka T, Mukuda T, Takase I, Kawahara A (2000a) Some factors affecting drinking behavior and their interactions in seawater-acclimated eels, *Anguilla japonica*. Zool Sci 17: 171-178

Ando M, Mukuda T, Takase I (2000b) Integrated aspects of osmoregulation in eels acclimated to sea water. Trends Comp Biochem Physiol 6: 85-94

Ando M, Nagashima K (1996) Intestinal Na^+ and Cl^- levels control drinking behavior in the seawater-adapted eel *Anguilla japonica*. J Exp Biol 199: 711-716

Aríëns-Kappers CU, Huber GC, Crosby EC (1936) "The Comparative Anatomy of the Nervous System of Vertebrates, Including Man. Vol 2" MacMilan, New York

Behred K, Donicht M (1990) Descending connections from the brainstem to the spinal cord in the electric fish *Eigenmannia*. Quantitative description based on retrograde horseradish peroxydase and fluorescent-dye transport. Brain Behav Evol 35: 227-239

Bourgue CW, Oliet HR, Richard D (1994) Osmoreceptors, osmoreception and osmoregulation. Front Neuroendocrinol 15: 231-274

Díaz-Regueira S, Anadón R (1992) Central projections of the vagus nerve in *Chelon labrosus* Risso (Teleostei, *O. Perciformes*). Brain Behav Evol 40: 297-310

Fitzsimons JT (1998) Angiotensin, thirst, and sodium appetite. Physiol Rev 78: 583-686

Goehler LE, Finger TE (1992) Functional organization of vagal reflex system in the brain stem of the goldfish, *Carassius auratus*. J Comp Neurol 319: 463-478

Hirano T (1974) Some factors regulating water intake by the eel, *Angulla japonica*. J Exp Biol 61: 737-747

Hlavacek M, Tahar M, Libouban S, Szabo T (1984) The mormyrid brainstem. I. Distribution of brain stem neurons projecting to the spinal cord in *Gnathonemus petersii*, an HRP study. J Hirnforsh 6: 603-615

Kanwal JS, Caprio J (1987) Central projections of the glossopharyngeal and vagal nerves in the channel catfish, *Ictalurus punctatus*: clues to differential processing of visceral inputs. J Comp Neurol 264: 216-230

Klüver H, Barrera E (1953) A method for the combined staining of cells and fibers in the nervous system. J Neuropathol Exp Neurol 12: 400-403

Kozaka T, Ando M (2003) Cholinergic innervation to the upper esophageal sphincter muscle in the eel, with special reference to drinking behavior. J Com Physiol B173: 135-140

Kozaka T, Fujii Y, Ando M (2003) Central effects of various ligands on drinking behavior in eels acclimated to seawater. J Exp Biol 206: in press

Martini FH, Timmons MJ, McKinley MP (2000) "Human Anatomy 3rd ed" Prentice Hall, New Jersey

Meek J, Nieuwenhuys R (1998) Holosteans and teleosts. In "The Central Nervous System of Vertebrates Vol. 2" ED by R Nieuwenhuys, HJ Ten Donkelaar, C Nicholson, Springer-Verlag, Berlin, pp 759-937

Meredith GE, Roberts BL (1986) The relationship of saccular efferent neurons to the superior olive in the eel, *Anguilla anguilla*. Neurosci Lett 68: 69-72

Meredith GE, Roberts BL (1987) Distribution and morphological characteristics of efferent neurons innervating end organs in the ear and lateral line of the European eel. J Comp Neurol 265: 494-506

Meredith GE, Roberts BL, Maslam S (1987) Distribution of afferent fibers in the brainstem from end organs in the ear and lateral line in the European eel. J Comp Neurol 265: 507-520

Molist P, Maslam S, Velzing E, Roberts BL (1993) The organization of the cholinergic neurons in the mesencephalon of the eel, *Anguilla anguilla*, as determined by choline acetyltransferase immunohistochemistry and acetylcholineesterase enzyme histochemistry. Cell Tissue Res 271: 555-566

Morita Y, Finger TE (1987a) Area postrema of the goldfish, *Carrasius auratus*: Ultrastructure, fiber connections, and immunocytochemistry. J Comp Neurol 256: 104-116

Morita Y, Finger TE (1987b) Topographic representation of the sensory and motor roots of the vagus nerve in the medulla of goldfish, *Carassius auratus*. J Comp Neurol 264: 231-249

Mukuda T, Ando M (2003) Medullary motor neurons associated with drinking behaviour of Japanese eels. J Fish Biol 62: 1-12

Nieuwenhuys R, Ten Donkelaar HJ, Nicholson C (1998) "The Central Nervous System of Vertebrates Vol. 2" Springer-Verlag, Berlin Heiderberg

Pérez SE, Yáñez J, Marin O, Anadón R, González A, Rodríguez-Moldes I (2000) Distribution of choline acetyltransferase (ChAT) immunoreactivity in the brain of the adult trout and tract-tracing observations on the connections of the nuclei of the isthmus. J Comp Neurol 428: 450-474

Peter RE, Gill VE (1975) A stereotaxic atlas and technique for forebrain nuclei of the goldfish, *Carassius auratus*. J Comp Neurol 159: 69-102

Roberts BL, Meredith GE, Maslam S (1989) Immunocytochemical analysis of the dopamine system in the brain and spinal cord of the European eel, *Anguilla anguilla*. Anat Embryol 180: 401-412

Takahashi A, Kishi E, Ishimaru H, Ikarashi Y, Maruyama Y (2001) Role of preoptic and anterior hypothalamic cholinergic input on water intake and body temperature. Brain Res 889: 191-199

Takei Y (2000) Comparative physiology of body fluid regulation in vertebrates with special reference to thirst regulation. Jpn J Physiol 50: 171-186

Takei Y, Hirano T, Kobayashi H (1979) Angiotensin and water intake in the Japanese eel, *Anguilla japonica*. Gen Comp Endocrinol 38: 183-88

Toga AW, Mazziotta JC (1996). "Brain Mapping. The Methods" Academic press , San Diego

Wullimann MF, Hofmann MH, Meyer DL (1991) Histochemical, connectional and cytoarchitectonic evidence for a secondary reduction of the pretectum in the European eel, *Anguilla anguilla*: A case of parallel evolution. Brain Behav Evol 38: 290-301

Wullimann MF, Rupp B, Reichert H (1996) "Neuroanatomy of the Zebrafish Brain: a Topological Atlas" Birkhauser Verlag , Switzerland

Zottoli SJ (1978) Comparison of Mauthner cell size in teleosts. J Comp Neurol 178: 741-758